

# Polymer Light-Emitting Electrochemical Cells: In Situ Formation of a Light-Emitting p–n Junction

Qibing Pei,\* Yang Yang, Gang Yu, Chi Zhang, and Alan J. Heeger

UNIAX Corporation, 6780 Cortona Drive, Santa Barbara, California 93117

Received November 2, 1995<sup>⊗</sup>

**Abstract:** Solid-state polymer light-emitting electrochemical cells have been fabricated using thin films of blends of poly(1,4-phenylenevinylene) and poly(ethylene oxide) complexed with lithium trifluoromethanesulfonate. The cells contain three layers: the polymer film (as the emissive layer) and indium–tin oxide and aluminum films as the two contact electrodes. When externally biased, the conjugated polymers are p-doped and n-doped on opposite sides of the polymer layer, and a light-emitting p–n junction is formed in between. The admixed polymer electrolyte provides the counterions and the ionic conductivity necessary for doping. The p–n junction is dynamic and reversible, with an internal built-in potential close to the band gap of the redox-active conjugated polymer (2.4 eV for PPV). Green light emitted from the p–n junction was observed with a turn-on voltage of about 2.4 V. The devices reached 8 cd/m<sup>2</sup> at 3 V and 100 cd/m<sup>2</sup> at 4 V, with an external quantum efficiency of 0.3–0.4% photons/electron. The response speed of these cells was around 1 s, depending on the diffusion of ions. Once the light-emitting junction had been formed, the subsequent operation had fast response (microsecond scale or faster) and was no longer diffusion-controlled.

## 1. Introduction

Conjugated polymers such as poly(1,4-phenylenevinylene) (PPV) have attracted attention since the discovery in the late 1970s that these polymers could be doped and the electric conductivity varied over the full range from insulator to metal.<sup>1–5</sup> They are semiconductors in the neutral nondoped state, and become highly conductive upon oxidation or reduction. Counterions are incorporated into the polymers during the oxidation–reduction process which is therefore a doping process, p-doping for oxidation and n-doping for reduction. This reversible electrochemical doping and the corresponding changes of the electrical, optical, and mechanical properties of the material have been exploited for a variety of applications such as rechargeable batteries, electrochromic windows, electrochemical “artificial muscles”, and sensors.<sup>6–10</sup> All these applications involve the use of a layer of conjugated polymer as

the working electrode in an electrochemical cell of the typical configuration with a liquid or solid electrolyte separating the working and auxiliary electrodes from each other.<sup>11</sup>

On the other hand, semiconducting conjugated polymers have been exploited for use in electronic and optical devices; these polymers have been successfully used as the active materials in field-effect transistors, light-emitting diodes, and polymer grid triodes.<sup>12–18</sup> Among these devices, the polymer-based light-emitting diodes (LEDs) are especially attractive for use in display technology. Polymer LEDs are constructed by sandwiching a layer of conjugated polymer between a pair of electrodes. When applying a high electric field between this pair of electrodes, electrons are injected from the cathode and holes are injected from the anode into the polymer layer. If

<sup>⊗</sup> Abstract published in *Advance ACS Abstracts*, April 15, 1996.

(1) For reviews, see: (a) Frommer, J. E.; Chance, R. R. in *Encyclopedia of Polymer Science and Engineering*; Grayson, M.; Kroschwitz, J., Eds.; Wiley: New York, 1986. (b) Skotheim, T. A., Ed. *Handbook of Conducting Polymers*; Marcel Dekker: New York, 1986. (c) Diaz, A. F.; Robinson, J. F.; Mark, H. B., Jr. *Adv. Polym. Sci.* **1988**, *84*, 113.

(2) (a) Chiang, C. K.; Fincher, C. R.; Park, Y. W.; Heeger, A. J.; Shirakawa, H.; Louis, E. J.; Gau, S. C.; MacDiarmid, A. G. *Phys. Rev. Lett.* **1977**, *39*, 1098. (b) Shirakawa, H.; Louis, E. J.; MacDiarmid, A. G.; Chiang, C. K.; Heeger, A. J. *J. Chem. Soc., Chem. Commun.* **1977**, 578. (c) Chiang, C. K.; Louis, E. J.; Druy, M. A.; Gau, S. C.; Heeger, A. J.; Louis, E. J.; MacDiarmid, A. G.; Park, Y. W.; Shirakawa, H. *J. Am. Chem. Soc.* **1978**, *100*, 1013.

(3) (a) Wnek, G. E.; Chien, J. C. W.; Karasz, F. E.; Lillia, C. P. *Polym. Commun.* **1979**, *20*, 1441. (b) Wegner, G.; Ruhe, J. *Faraday Discuss. Chem. Soc.* **1989**, *88*, 333. (c) Baughman, R. H.; Murthy, N. S.; Eckhardt *Phys. Rev. B: Condens. Matter* **1992**, *46*, 10515.

(4) (a) Kanazawa, K. K.; Diaz, A. F.; Geiss, R. F.; Gill, W. D.; Kwak, J. F.; Logan, J. A.; Rabolt, J. F.; Street, G. B. *J. Chem. Soc., Chem. Commun.* **1979**, 854. (b) Bull, R. A.; Fan, F. R. F.; Bard, A. J. *J. Electrochem. Soc.* **1982**, *129*, 1009. (c) Burgmayer, P.; Murray, R. W. *J. Phys. Chem.* **1984**, *88*, 2515. (d) Krishna, V.; Ho, Y. H.; Basak, S.; Rajeshwar, K. *J. Am. Chem. Soc.* **1991**, *113*, 3325.

(5) (a) Kaufman, J. H.; Kanazawa, K. K.; Street, G. B. *Phys. Rev. Lett.* **1984**, *53*, 2461. (b) Orata, D.; Buttry, D. J. *Am. Chem. Soc.* **1987**, *109*, 3574. (c) Prezyna, L. A.; Qiu, Y. J.; Reynolds, J. R.; Wnek, G. E. *Macromolecules* **1991**, *24*, 5283. (d) Pei, Q.; Ingnas, O. *J. Phys. Chem.* **1992**, *96*, 10507. (e) Pei, Q.; Ingnas, O. *J. Phys. Chem.* **1993**, *97*, 6034.

(6) Nigrey, P. J.; MacInnes, D.; Nairns, D. P.; MacDiarmid, A. G.; Heeger, A. J. *J. Electrochem. Soc.* **1981**, *128*, 1651.

(7) Shacklette, L. W.; Maxfield, M.; Gould, S.; Wolf, J. F.; Jow, T. R.; Baughmann, R. H. *Synth. Met.* **1987**, *18*, 611.

(8) Garnier, F.; Tourillon, G.; Gizard, M.; Dubois, J. C. *J. Electroanal. Chem.* **1983**, *148*, 299.

(9) (a) Pei, Q.; Ingnas, O. *Adv. Mater.* **1992**, *4*, 277. (b) Pei, Q.; Ingnas, O.; Lundstrom, I. *Smart Mater. Struct.* **1993**, *2*, 1.

(10) (a) Nylander, C.; Armgarth, M.; Lundström, I. *Proceedings of the International Meeting on Chemical Sensors*, Fukuoka, Japan, 1983; p 203. (b) Gustafsson, G.; Lundström, I.; Liedberg, B.; Ingnäs, O.; Wennerström, O. *Synth. Met.* **1989**, *31*, 163. (c) Pei, Q.; Qian, R. *Electrochim. Acta* **1992**, *37*, 1075.

(11) Bard, A. J.; Faulkner, L. R. *Electrochemical Methods: Fundamentals and Applications*; Wiley: New York, 1980.

(12) (a) Garnier, F.; Peng, F. Z.; Horowitz, G.; Fichou, D. *Adv. Mater.* **1990**, *2*, 592. (b) Garnier, F.; Hajlaoui, R.; Yassar, A. *Science* **1994**, *265*, 1684.

(13) Assadi, A.; Svenson, C.; Willander, M.; Ingnas, O. *Appl. Phys. Lett.* **1988**, *53*, 195.

(14) Dodabalapur, A.; Torsi, L.; Katz, H. E. *Science* **1995**, *268*, 270.

(15) (a) Burroughes, J. H.; Bradley, D. D. C.; Brown, A. R.; Marks, R. N.; Mackay, K.; Friend, R. H.; Burns, P. L.; Holmes, A. B. *Nature* **1990**, *347*, 539. (b) Burn, P. L.; Holmes, A. B.; Kraft, A.; Bradley, D. D. C.; Brown, A. R.; Friend, R. H.; Gymer, R. W. *Nature* **1992**, *356*, 47.

(16) (a) Braun, D.; Heeger, A. J. *Appl. Phys. Lett.* **1991**, *58*, 1982 (1991). (b) Gustafsson, G.; Cao, Y.; Treacy, G. M.; Klavetter, F.; Colaneri, N.; Heeger, A. J. *Nature* **1992**, *357*, 477.

(17) (a) Grem, G.; Leditzky, G.; Ullrich, B.; Leising, G. *Adv. Mater.* **1992**, *4*, 36. (b) Grem, G.; Leising, G. *Synth. Met.* **1993**, *55–57*, 4105. (c) Yang, Z.; Sokolik, I.; Karasz, F. E. *Macromolecules* **1993**, *26*, 1188.

(18) Yang, Y.; Heeger, A. J. *Nature* **1995**, *372*, 344.

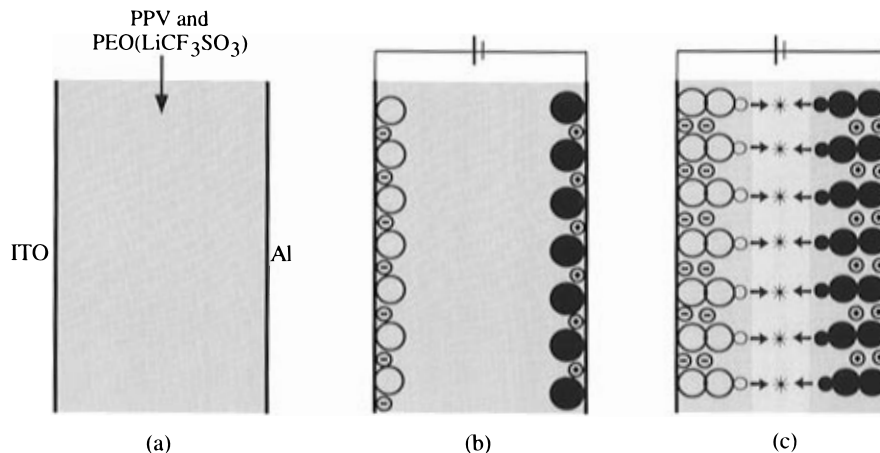


**Figure 1.** Schematic diagram of the electrochemical processes in a solid-state light-emitting electrochemical cell: (large open circle) an oxidized molecule, (large closed circle) a reduced molecule, (circled minus) an anion, (circled plus) a cation, (small open circle) a hole, (small closed circle) an electron, (asterisk) a photon. This figure, presented here in black and white, is available in color on the World Wide Web. See Supporting Information paragraph on any current masthead page for instructions on accessing the images.

the polymer is fluorescent, the injected electrons and holes recombine radiatively, yielding electroluminescence.

Recently, the invention of a new type of light-emitting device has been reported;<sup>19,20</sup> the light-emitting electrochemical cell (LEC) combines the novel electrochemical properties of conjugated polymers with the ionic conductivity of polymer electrolytes. In these solid-state LECs, the conjugated polymers are p-doped on the anode side and n-doped on the cathode side and a light-emitting p–n junction is formed between the p-doped and n-doped regions. In this paper, we describe the electrochemical operating mechanism of LECs, and we discuss the fundamental issues associated with the reversible formation of the light-emitting p–n junction. For these studies, we have used poly(1,4-phenylenevinylene), PPV, admixed with a polymer electrolyte as the electrochemically active layer.

## 2. Mechanism of Operation of the Solid-State LEC

Figure 1 is a schematic diagram of the LEC. Between the two contact electrodes (ITO and Al) is a layer of poly(1,4-phenylenevinylene) (PPV) admixed with a complex of poly(ethylene oxide) (PEO) and lithium trifluoromethanesulfonate. PPV is a luminescent polymer which can be electrochemically doped n-type or p-type, and PEO complexed with a lithium salt is a polymer electrolyte with relatively high ionic conductivity. When a sufficiently high voltage is applied between ITO and Al, charge is injected from the electrodes into PPV. Assuming that the ITO electrode is wired as the anode and the Al electrode as the cathode, the PPV polymer near the ITO is initially oxidized, the polymer near Al is reduced (Figure 1b), and counterions from the electrolytes move to compensate the charges on the oxidized and reduced polymer chains. Since both p- and n-doped PPV are good electronic conductors, the PPV/electrode interfaces consequently become low-resistant contacts.

The simultaneous p-doping and n-doping are initiated by setting the electrochemical potential at the HOMO (top of the  $\pi$ -band) of the conjugated polymer on the anode side, and at the LUMO (bottom of the  $\pi^*$ -band) on the cathode side. The minimum bias voltage ( $V_{on}$ ) to do so is the difference ( $E_g$ ) in chemical potentials between the LUMO and HOMO:

$$eV_{on} = E_g \quad (1)$$

At bias voltages higher than  $V_{on}$ , the redox reactions (with

associated counterion insertion) symmetrically dope the PPV near the ITO and Al electrodes to higher levels.

In general, the current passing through the LEC is made up of two components: an ionic contribution and an electronic contribution. After changing the applied voltage, oxidation and reduction will occur and ions will move (i.e., the corresponding doping levels will adjust) until the cell is in electrochemical equilibrium. After forming the p–n junction and coming to electrochemical equilibrium at an applied voltage greater than  $V_{on}$ , the ionic contribution to the current goes to zero. The electronic contribution to the current does not go to zero: under the influence of the applied voltage the holes in the  $\pi$ -band of PPV (p-type carriers) propagate from the anode toward the cathode, and the electrons in the  $\pi^*$ -band (n-type carriers) propagate from the cathode toward the anode. These holes and electrons meet in the compensated volume between the n-type-doped and p-type-doped regions; this compensated volume defines the electrochemically induced p–n junction. Within this p–n junction, the p-type and n-type carriers recombine to form neutral charge carrier pairs which radiatively decay to the ground state. Although the width and shape of the p–n junction are not yet understood in detail (for example, as a function of the bias voltage), on general grounds we expect the doped regions to extend more deeply into the polymer at higher bias voltages with an associated narrowing of the p–n junction.

The electrochemically induced p–n junction is dynamic and reversible. The direction of the p–n junction can be reversed simply by wiring ITO as the cathode and Al as the anode. Alternatively, the junction can be removed by discharging the previously charged electrochemical cell; this discharge can be carried out either with the two contact electrodes shorted or with the cell in open circuit conditions. In the latter case, the discharge current flows internally through the semiconducting polymer; in short circuit conditions, the discharge current flows primarily in the external circuit (since the external impedance can be made much less than the internal resistance of the conducting polymer layer). Under such short circuit discharge conditions, the integrated current provides an estimate of the doping level:

$$Q = \int i(t) dt \quad (2)$$

The doping concentration (charge per repeating unit of the redox

(20) Pei, Q.; Yu, G.; Zhang, C.; Yang, Y.; Heeger, A. J. *Science* **1995**, *269*, 1086.

(19) Pei, Q.; Klavetter, F. US Patent Appl. No. 08/268763, June 28, 1994.

polymer) is, therefore,

$$c \approx Q/eN \quad (3)$$

where  $N$  is the number of repeat units of the redox polymer in the film. Although the equality in eq 3 is only approximate (the compensated region within the p–n junction is not doped), this relation can be used to obtain an estimate of the doping level and to demonstrate that the LEC functions as a charged electrochemical cell which can store both charge and energy.

Because the electrical conductivity of the conducting polymer increases by many orders of magnitude upon p-type or n-type doping, most of the external bias is applied across the p–n junction. Therefore, the minimum bias to maintain the p–n junction equals the built-in potential difference of the p–n junction which is ideally equal to the LUMO–HOMO band gap of the redox material divided by the elementary charge ( $E_g/e$ ). A bias voltage higher than  $E_g/e$  will initiate the flow of electrons and holes into the p–n junction with concurrent light emission. In principle, the turn-on and operating voltages of LECs are not sensitive to the total thickness of the polymer layer. If, however, the thickness is too great or if the electronic mobility is too low (as for example at low temperatures), the series resistance of the n-type- and p-type doped regions will decrease the actual voltage applied across the junction and the device will require higher operating voltage.

### 3. LECs, Electrochemiluminescent Cells, and Polymer LEDs: Comparisons

Unlike polymer light-emitting diodes (LEDs) which utilize the semiconductor properties of nondoped conjugated polymers and conventional electrochemical cells (batteries) which utilize the redox properties of these polymers, LECs utilize both the semiconductor properties and the redox properties. The high electronic conductivity of conjugated polymers after doping is also essential to the operation of LECs.

Electroluminescence from electrochemical cells, known as electrochemiluminescence, has been known for many years.<sup>21–24</sup> However, the mechanism of electroluminescence operating in LECs is fundamentally different from the phenomena associated with electrochemiluminescence. Electrochemiluminescent devices rely on transport of the oxidized or reduced light-emitting molecules (ions) themselves through the electrolyte between the electrodes, rather than transport of the electronic charge carriers between the electrodes. The oxidized and reduced species (ions) then react with each other (or the electrode) to form the original organic or metalloorganic species in an excited state which can subsequently decay radiatively. Electrochemiluminescent displays have been described in which the electrochemiluminescent substance is dissolved in a solid electrolyte. Nevertheless, after generation of the oxidized and reduced species, the ions diffuse away from their respective electrodes and eventually meet somewhere between the two electrodes. Since the diffusion of the ions is slow, the current and the intensity of light emission are low. Alternatively, electrochemiluminescent material can be fixed on one of the electrodes in an electrochemical cell and cyclically reduced and oxidized by an alternating potential. A direct current potential can be used

only if the cell contains an additional species which serves to interact with the luminescent material in such a way as either to oxidize the electrochemically reduced material to the neutral excited state or to reduce the electrochemically oxidized material to the neutral excited state.

In the LEC, on the other hand, the oxidized and reduced macromolecules are immobile; they do not physically move from one electrode to the other. On the contrary, it is the electrons in the  $\pi^*$ -band and the holes in the  $\pi$ -band (i.e., the electronic charge carriers) which move between the electrodes within the immobile semiconductor. As noted above, ions move only during the transient formation of the p–n junction. Ion transport is not directly involved in the light emission; after reaching a steady state under a fixed applied voltage, all ion transport stops. Under such steady-state conditions, electrons from the n-type region and holes from the p-type region combine in the compensated p–n junction to form neutral pairs which radiatively decay and give off light.

Electrochemical systems have been studied where redox active molecules were dissolved in solid polymer electrolytes.<sup>25</sup> Electrochemical reactions of the redox molecules in the bulk polymer phase occur via the diffusion of the redox molecules to electrodes. Although electron hopping between redox centers in these systems sometimes plays a role in charge transport, both the mass transport of the redox molecules and the electron hopping are slow. The diffusion-type cyclic voltammograms indicate that even the faster of the two processes had a narrow diffusion distance, probably limited to the regions near the electrode interfaces. Therefore, no p–n junction was formed in such solid electrochemical systems. On the contrary, as will be shown below, once the light-emitting p–n junction has been formed in an LEC, the electronic charge injection into the polymer layer is no longer diffusion controlled.

LEC devices also differ from conventional polymer LEDs (and organic LEDs as well). In contrast to LECs, LEDs have no ionic species in the polymer layer to compensate for the charges on the polymer chains. In the LED, the semiconducting polymer layer is oxidized on one side (holes are injected) and reduced on the other side (electrons are injected), but doping does not take place. The electrons and holes are injected by tunneling through the energy barriers formed at the electrode/polymer interfaces. Consequently, low-work-function cathodes, and high-work-function anodes are usually required to produce bright and efficient light emission.<sup>26–28</sup> The fundamental difference between the operating mechanisms of polymer LEDs and polymer LECs demonstrates clearly and unambiguously the difference between redox and doping in conducting polymers.

### 4. Experimental Details

Poly(1,4-phenylenevinylene) is prepared by the precursor route.<sup>29,30</sup> The precursor poly(xylylidene-tetrahydrothiophenium chloride) was prepared according to ref 30d. Poly(ethylene oxide) (PEO),  $M_w = 5\,000\,000$ , was purchased from Polysciences. Lithium trifluoromethane-

(21) Faulkner, L. R.; Bard, A. J. in *Electroanalytical Chemistry*; Bard, A. J., Ed.; Marcel Dekker: New York; 1977; Vol. 10, pp 1–95.

(22) Brilmyer, G. H.; Bard, A. J. *J. Electrochem. Soc.* **1980**, *127*, 104. (b) Rubinstein, I.; Bard, A. J. *J. Am. Chem. Soc.* **1980**, *102*, 6641. (c) Fan, F. R. F.; Mau, A.; Bard, A. J. *Chem. Phys. Lett.* **1985**, *116*, 400.

(23) Bartelt, J. E.; Drew, S. M.; Wightman, R. M. *J. Electrochem. Soc.* **1992**, *139*, 70.

(24) Richter, M. M.; Fan, F. R. F.; Klavetter, F.; Heeger, A. J.; Bard, A. J. *Chem. Phys. Lett.* **1994**, *226*, 115.

(25) Ruff, I.; Botar, L. *J. Chem. Phys.* **1985**, *83*, 1292. (b) Geng, L.; Longmire, M. L.; Reed, R. A.; Kim, M. H.; Wooster, T. T.; Oliver, B. N.; Egekeze, J.; Kennedy, R. T.; Jorgenson, J. W.; Parcher, J. F.; Murray, R. W. *J. Am. Chem. Soc.* **1989**, *111*, 1619. (c) Watanabe, M.; Wooster, T. T.; Murray, R. W. *J. Phys. Chem.* **1991**, *95*, 4573. (d) Watanabe, M.; Nagasaka, H.; Sanui, K.; Ogata, N.; Murray, R. W. *Electrochim. Acta* **1992**, *37*, 1521. (e) Valazquez, C. S.; Hatchison, J. E.; Murray, R. W. *J. Am. Chem. Soc.* **1993**, *115*, 7896. (f) Watanabe, M.; Nagasaka, H.; Ogata, N. *J. Phys. Chem.* **1995**, *99*, 12294.

(26) Brown, A. R.; Bradley, D. D. C.; Burn, P. L.; Burroughes, J. H.; Friend, R. H.; Greenham, N. C.; Holmes, A. B.; Kraft, A. *Appl. Phys. Lett.* **1992**, *61*, 2793.

(27) Parker, I. D. *J. Appl. Phys.* **1994**, *75*, 1656.

(28) (a) Parker, I. D.; Pei, Q.; Marrocco, M. *Appl. Phys. Lett.* **1994**, *65*, 1272. (b) Pei, Q.; Yang, Y. *Chem. Mater.* **1995**, *7*, 1568.

sulfonate ( $\text{LiCF}_3\text{SO}_3$ ) was purchased from Aldrich. Both PEO and  $\text{LiCF}_3\text{SO}_3$  were used without further treatment. Thin polymer films were prepared by spin-casting from a solution containing 50 mg of poly(xylylidene-tetrahydrothiophenium chloride), 50 mg of PEO, and 8.9 mg of  $\text{LiCF}_3\text{SO}_3$  dissolved in 10 mL of acetonitrile. A small amount of water was added in the solution to enhance codissolution of the two polymers. The molar ratio of  $\text{LiCF}_3\text{SO}_3$  to the  $\text{CH}_2\text{CH}_2\text{O}$  moieties in PEO was 1:20.<sup>31</sup> The spinning rate was 800 rpm. The films were then heated in a nitrogen atmosphere at 200 °C for 3 h to convert the precursor polymer into PPV.

LEC devices were fabricated on a transparent, indium–tin oxide (ITO) coated glass substrate (purchased from Standish) in a drybox. Thin films of the PPV and PEO( $\text{LiCF}_3\text{SO}_3$ ) blend were used as the active light-emitting layer between ITO and aluminum electrodes (the 400 Å Al layer was evaporated onto the polymer film at pressures around  $1 \times 10^{-6}$  Torr). The polymer layer was typically 0.4  $\mu\text{m}$  thick. The LECs fabricated with this structure are denoted by the abbreviation ITO/PPV + PEO/Al. The active area of the devices was 12 mm<sup>2</sup>. The devices were tested in a drybox. The yield of the devices was above 90%. For convenience, the forward voltage bias below indicates that the ITO electrode is wired as the anode.

UV–vis absorption spectra were recorded using an HP 8452A diode array UV–vis spectrophotometer. Photoluminescent and electroluminescent spectra were obtained using an Oriel Multispec 4 CCD array spectrometer.

## 5. Results and Discussion

**5.1. PPV + PEO( $\text{LiCF}_3\text{SO}_3$ ) Blends.** For these initial studies, we chose poly(1,4-phenylenevinylene) (PPV) and poly(ethylene oxide) (PEO) as the electronic and ionic conductors, respectively. Both PPV and PEO are representative in their category. PPV is a conjugated polymer capable of both p- and n-type doping. The conductivity of neutral (non-doped) PPV is less than  $10^{-12}$  S/cm at room temperature.<sup>30b</sup> Both p-doped and n-doped PPVs are highly conductive (measurements of n-type material are more difficult because of the reactivity of the n-type material with moisture and oxygen).<sup>32</sup> Furthermore, pure PPV is fluorescent, with efficient green emission, while in doped PPV, the luminescence is quenched.<sup>33</sup> PEO is a known ionic conductor. When complexed with a lithium salt, especially with a plasticizing salt such as  $\text{LiCF}_3\text{SO}_3$ , the ionic conductivity is as high as  $10^{-6}$  S/cm at room temperature, increasing to  $10^{-4}$  S/cm at 72 °C.<sup>31c</sup>

Thin films of PPV + PEO( $\text{LiCF}_3\text{SO}_3$ ) blends have an ionic conductivity of  $\sim 1 \times 10^{-7}$  S/cm at 22 °C, and  $\sim 1 \times 10^{-5}$  S/cm at 80 °C. The PPV + PEO( $\text{LiCF}_3\text{SO}_3$ ) films also retain the characteristics of PPV: (i) In the nondoped, pristine form, they are photoluminescent, emitting green light with the spectrum

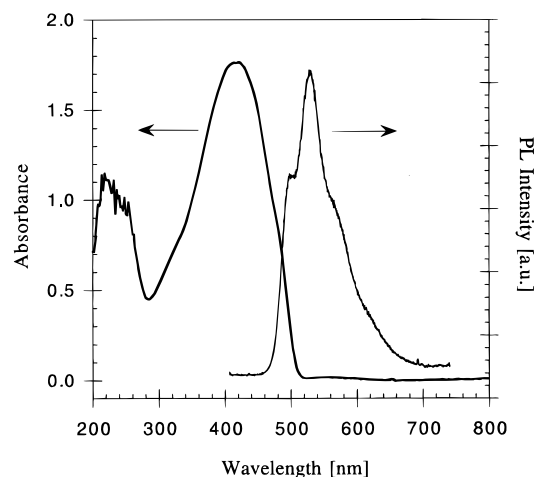


**Figure 2.** Optical absorption and photoluminescent spectra of a thin layer of a blend of PPV and PEO with  $\text{LiCF}_3\text{SO}_3$  in the ratio of 1:1:0.18 by weight.

characteristic of PPV. (ii) Such films can be doped and become highly conductive ( $\sigma > 1$  S/cm) after being exposed to iodine.

Although doped PPV is not fluorescent, a blend of PPV containing ionic species, but without oxidative or reductive doping, retains the fluorescence of pure PPV. Electron microscopy studies have shown that the blends are phase-separated composites, as would be expected from mixtures of polar and nonpolar polymers, each with relatively high molecular weight. The ions are, therefore, compensated in pairs and stored primarily in the PEO.<sup>31,32</sup>

The morphology of the PPV + PEO( $\text{LiCF}_3\text{SO}_3$ ) blend films could be changed simply by changing the water content in the solution used to cast the films. In anhydrous acetonitrile, the PPV precursor precipitated from the solution upon mixing with the PEO( $\text{LiCF}_3\text{SO}_3$ ) solution. In aqueous solution with less than 50% acetonitrile, the high molecular weight PEO( $\text{LiCF}_3\text{SO}_3$ ) precipitated. The optimal water:acetonitrile ratio of solution was found to be around 1:5 by volume which was used in this study. Higher and lower water contents both induced macroscopic phase separation ( $> 0.1 \mu\text{m}$ ) in the spin-cast films and lowered device performance (higher leakage current, lower quantum efficiency, and slower response). Moisture was removed from the blend films during the conversion of the precursor polymer to PPV.

The UV–vis absorption and photoluminescent spectra of a PPV + PEO( $\text{LiCF}_3\text{SO}_3$ ) film are displayed in Figure 2. The absorption onset is at 515 nm, which corresponds to a LUMO–HOMO band gap ( $E_g$ ) of 2.4 eV; the absorption peak is at 415 nm. The photoluminescent spectrum has a strong peak at 530 nm, with shoulders on both sides. These spectral features are in good agreement with pure PPV film converted from the precursor at temperatures  $\geq 200$  °C.

Since the PPV + PEO( $\text{LiCF}_3\text{SO}_3$ ) films retain both the characteristics of the PEO( $\text{LiCF}_3\text{SO}_3$ ) complex and PPV, a phase-separated interpenetrating polymer network is probably formed in the blend films. While the PEO network provides the channels for ion transport, the PPV network provides the pathways for transport of electronic charge carriers. The interpenetrating polymer network is an attractive morphology for the active material in the polymer-based solid-state light-emitting electrochemical cells.

**5.2. Current–Light–Voltage characteristics of an LEC.** When an external voltage was applied to an ITO/PPV + PEO/Al sandwich structure, light was emitted from the polymer layer. Figure 3 shows typical current–light–voltage characteristics

(29) Wessling, R. A. *J. Polym. Sci. Polym. Symp.* **1985**, 72, 55.

(30) (a) Gagnon, D. R.; Capistran, J. D.; Karasz, F. E.; Lenz, R. W. *Polym. Prepr.* **1984**, 25, 284. (b) Bradley, D. D. C. *J. Phys. D: Appl. Phys.* **1987**, 20, 1389. (c) Gmeiner, J.; Karg, S.; Meier, M.; Riess, W.; Strohrriegel, P.; Schwoerer, M. *Acta Polym.* **1993**, 44, 201. (d) Burn, P. L.; Bradley, D. D. C.; Friend, R. H.; Halliday, D. A.; Holmes, A. B.; Jackson, R. W.; Kraft, A. *J. Chem. Soc., Perkin Trans. 1* **1992**, 3225.

(31) (a) Wright, P. V. *Br. Polym. J.* **1975**, 7, 319. (b) Armand, M. B.; Chabagno, J. M.; Duclot, M. *Extended Abstracts of the 2nd International Meeting on Solid Electrolytes*, St. Andrews, Scotland, Sept. 20–22, 1978. (c) Walker, C. W., Jr.; Salomon, M. J. *Electrochem. Soc.* **1993**, 140, 3409.

(32) (a) Murase, I.; Ohnishi, T.; Noguchi, T.; Hirooka, M.; Murakami, S. *Mol. Cryst. Liq. Cryst.* **1985**, 118, 333. (b) Schlenoff, J. B.; Obrzut, J.; Karasz, F. E. *Phys. Rev. B: Condens. Matter* **1989**, 40, 11822. (c) Mertens, R.; Nagels, P.; Callaerts, R.; Van Roy, M.; Briers, J.; Geise, H. J. *Synth. Met.* **1992**, 51, 55.

(33) (a) Capistran, J. D.; Gagnon, D. R.; Antoun, S.; Lenz, R. W.; Karasz, F. E. *Polym. Prepr.* **1984**, 25, 282. (b) Hayashi, S.; Kaneto, K.; Yoshino, K. *Solid State Commun.* **1987**, 61, 249. (c) Bradley, D. D. C.; Friend, R. H. *J. Phys. Condens. Matter* **1989**, 1, 3671. (d) Eckhardt, H.; Shacklette, L. W.; Jen, K. Y.; Elsenbaumer, R. L. *J. Chem. Phys.* **1989**, 91, 1303. (e) Dyreklev, P.; Inganas, O.; Paloheimo, J.; Stubb, H. *J. Appl. Phys.* **1992**, 71, 2816. (f) Yoshino, K.; Yin, X. H.; Muro, K.; Kiyomatsu, S. *Jpn. J. Appl. Phys., Part 2* **1993**, 32, L357.

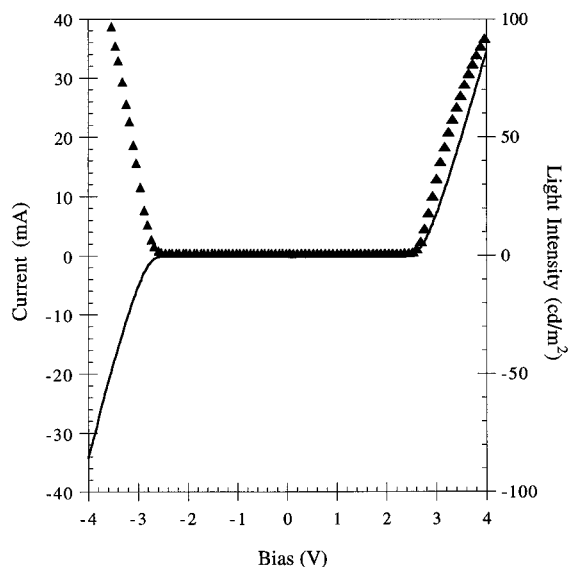


**Figure 3.** Typical current–light–voltage characteristics of an ITO/PPV + PEO(Li)/Al cell. The voltage scans from 0 to 4 V and from 0 to –4 V, respectively.

of an ITO/PPV + PEO/Al cell under both forward and reverse bias conditions. The current–voltage curve is antisymmetric about the origin, in contrast to conventional semiconductor diodes where a large rectification ratio (ratio of forward to reverse current) on the order of  $10^3$ – $10^8$  is obtained. In the LEC, the rectification ratio is near unity. The light–voltage curve is symmetric about zero bias. The apparent threshold voltages for appreciable current injection and visible light emission are at 2.5 V for forward voltage scans sweeping from 0 to 4 V, and around –2.6 V for reverse scans sweeping from 0 to –4 V. These threshold voltages are very close to the optical band gap of PPV (2.4 eV).

The threshold voltages increase slightly with thicker polymer films, but the increase is much less significant than that in conventional polymer light-emitting diodes where the threshold voltage is roughly proportional to the thickness of the electroluminescent layer.<sup>27</sup> This small thickness dependence of the threshold voltage results from a combination of the limited ionic conductivity ( $10^{-7}$  S/cm) and the series resistance of the lightly doped material.

The low mobility of the counterions delays the formation of the light-emitting p–n junction in thicker films. This effect is clearly seen when the voltage scan is carried out at various sweep rates as shown in Figure 4. The apparent threshold voltage increases with sweep rate, characteristic of an electrochemical process during linear sweep voltammetry. The expected hysteresis resulting from the low ionic mobility is shown in Figure 5. The light–voltage curve during a forward scan (sweep from 0 to 4 V) shows a shift of the threshold voltage by about 0.2 V upfield compared to the curve during the reverse scan (sweep from 4 to 0 V). During the reverse scan sweeping from 4 to 0 V, a peak is observed at about 3.5 V. The time interval from the beginning of the sweep to the peak position is about 10 s. This interval reflects the time scale to form the p–n junction in this system. The hysteresis can be reduced and made negligible by decreasing the sweep rate.

Under a constant voltage of 4 V, the devices turned-on (started emitting light) in less than 0.1 s. The current and light intensity continued to increase for about 10 s when the p–n junction reached equilibrium. Once the junction had been formed, the subsequent operation had fast response (microsecond scale or faster).

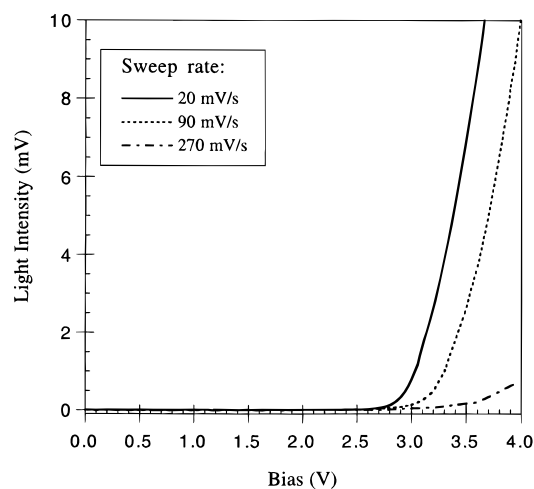


**Figure 4.** Light–voltage characteristics of an ITO/PPV + PEO(Li)/Al cell during voltage scans from 0 to 4 V at sweep rates of 20, 90, and 270 mV/s.

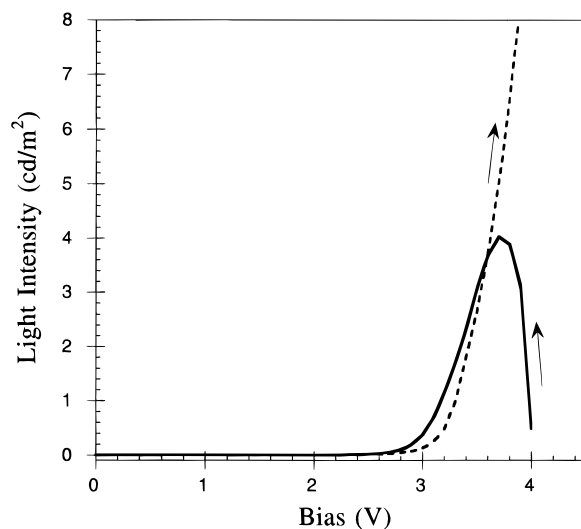


**Figure 5.** Light–voltage characteristics of an ITO/PPV + PEO(Li)/Al cell during a forward scan (0 → 4 V) and a reverse scan (4 → 0 V) at a sweep rate of 90 mV/s.

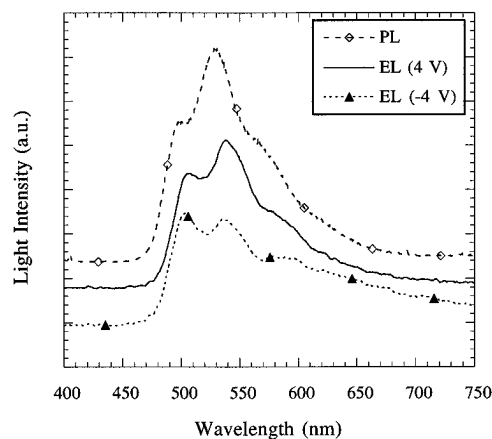


**Figure 6.** Electroluminescent and photoluminescent spectra of a thin layer of a blend of PPV and PEO with  $\text{LiCF}_3\text{SO}_3$  in the ratio of 1:1:0.18. The electroluminescent spectra were generated by incorporation of the layer in an ITO/PPV + PEO/Al LEC structure.

Figure 6 displays the electroluminescent spectra of the green light emitted from devices operated at +4 and –4 V. Both spectra are close to the photoluminescent spectrum of the polymer layer (PPV is the chromophore), confirming the

expected reversible formation of the junction. Photons are generated by the radiative recombination of holes in the HOMO and electrons in the LUMO of PPV. The slight change of the relative intensity of the emission peaks has also been observed in light-emitting diodes using pure PPV as the emissive layer, and attributed to the self-absorption of PPV.<sup>37</sup>

Initial stress life results are promising: devices were continuously stressed at +4 and -4 V (light intensity about 100 cd/m<sup>2</sup>) for 24 h, with a loss of emission intensity by less than 50%. At lower light output, the stress life is significantly longer. For example, at +3 and -3V bias (about 8 cd/m<sup>2</sup>), the light intensity decays by only 5% in 24 h. In addition, since stable metals are used as the contact electrodes, and the fluorescent conjugated polymers are in their neutral undoped form, all components of the LECs are environmentally stable at the quiescent "off" state. As a result, one anticipates intrinsically longer storage lifetime. Our initial ITO/PPV + PEO/Al devices have been stored in an argon atmosphere for 15 months. After such long-term storage, the devices operate without loss of efficiency and do not exhibit the formation of black spots which typically limit the storage lifetime of polymer LEDs.

### 5.3. Doping and p-n Junction Formation in LECs.

Because the polymer must be symmetrically p- and n-doped on opposite sides of the polymer layer, light is emitted from the p-n junction which will form between the two electrodes. Although the same charge must be injected at both electrodes (positive on one side and negative on the other), the polymer need not be precisely electron-hole symmetric. Thus, one doping type (e.g., n-type) could occupy a larger volume at a lower doping concentration than the other (e.g., p-type).

To investigate the location and width of the light-emitting junction, we fabricated LECs in a surface cell configuration.<sup>35</sup> A thin layer of PPV + PEO(LiCF<sub>3</sub>SO<sub>3</sub>) was spin-cast onto a glass substrate prepared with parallel, interdigitated gold electrodes (Figure 7, the black lines). The gold electrodes in Figure 7 are 50 μm wide; the spacing between the electrodes is 15 μm. When 4 V was applied between the two electrodes, a yellow-green emission line near the center of the spacing was clearly seen after an induction period of about 1 min. The photo displayed in Figure 7 shows the emission line, which defines the dynamically formed p-n junction. In Figure 7, the junction is relatively straight; the wavy structure noted earlier<sup>20</sup> was possibly the result of nonuniformity in the polymer layer. Because a p-n junction is a capacitor, the energy stored in the junction ( $CV^2/2$  per unit volume) is proportional to its length. Thus, the stored energy functions as a source of line tension which tends to suppress deviations from straight line behavior.

The width of the p-n junction in Figure 7 is approximately 1–3 μm within the 15 μm wide spacing. The junction is slightly closer to the anode than to the cathode. In addition, the area between the anode and the emission line is darker than the area between the emission line and the cathode, consistent with p-type doping to a higher level in a smaller volume. During a period of continuous operation, the dark area slowly grew, pushing the junction closer to the cathode. The width of the light-emitting junction remained essentially constant. Why the p-n junction moved toward the cathode remains an open question.

When a high voltage, e.g., 25 V, was applied between the two parallel gold electrodes, light was emitted from the entire spacing between the electrodes. The bright area rapidly narrowed and became a narrow line near the center of the interelectrode spacing in a few seconds. However, when the device was operated at a low voltage, such as 4 V, no light was

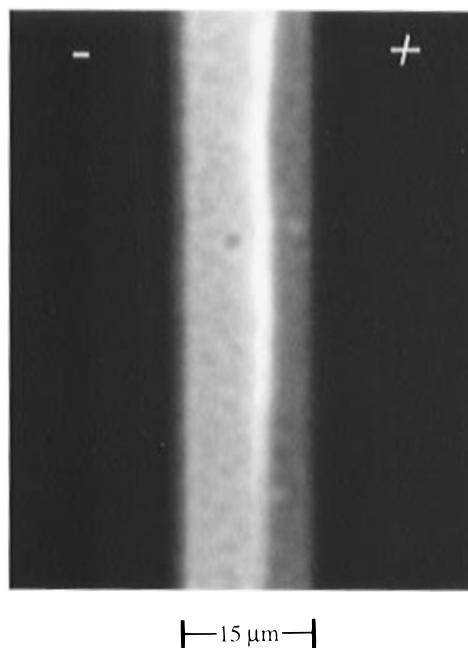


**Figure 7.** An optical microphotograph of the Au/PPV + PEO/Au LEC (surface cell configuration) during operation. A 4 V bias is being applied between the pair of gold electrodes which are separated by 15 μm. Green light is emitted from the narrow p-n junction near the center of the spacing. This figure, presented here in black and white, is available in color on the World Wide Web. See Supporting Information paragraph on any current masthead page for instructions on accessing the images.

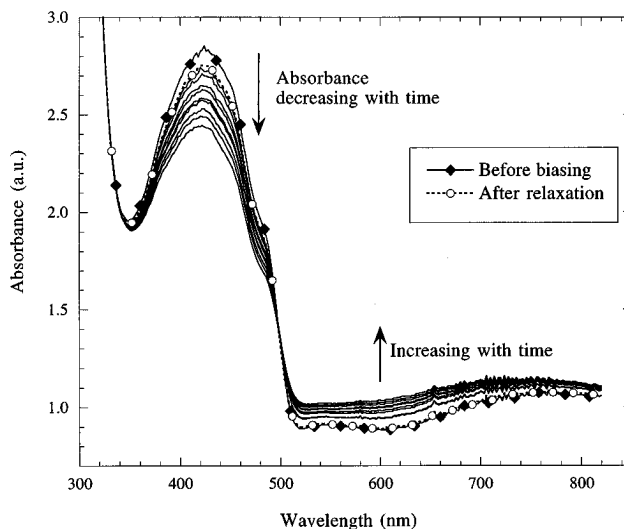


**Figure 8.** Absorption spectra of an ITO/PPV + PEO/Al cell during operation at 6 V. The Al layer is 100 Å thick and is semitransparent. Key: (◆) the fresh cell before being biased, (—) biased at 6 V as a function of time (spectra were taken at 1 min intervals), (○) zero bias, 2 min after the last operation.

observable before the narrow light-emitting junction was formed after about 1 min.

In order to obtain some initial information on the in situ doping, an ITO/PPV + PEO/Al sandwich structure was fabricated, and the optical absorption spectrum of the LEC was measured during light emission. The Al layer was 100 Å thick and semitransparent. The absorption spectra of the device during operation at 6 V are displayed in Figure 8 (since the thin Al layer had higher resistance, a higher voltage was required to gain light emission visible to the naked eye). Green light was emitted from the device. At the same time, the absorption

spectrum of the polymer layer changed. The intensity of the absorption peak due to the HOMO–LUMO band gap transition decreases, and its position slightly blue shifts with increasing time, while the absorption in the red–near-infrared regime increases. This process is reversible. As the bias is reduced to 0 V, the spectrum gradually returns to that of the pure polymer. This spectral development is consistent with the expected electrochemical doping of PPV. The weak absorption in the red–near-infrared regime suggests that, in the sandwich cell, the PPV is relatively lightly doped. In the sandwich structure, where the active polymer layer is less than 1  $\mu\text{m}$  thick, the width of the p–n junction might be close to the thickness of the polymer layer. In this situation, therefore, a relatively small spectral change would be expected, as indicated in Figure 8. The doping level in the p-type and n-type regions and the profile of the p–n junction is clearly dependent on the interelectrode spacing (in the surface cell, the junction is 1–3  $\mu\text{m}$ , considerably wider than the thickness of the entire layer in the sandwich cell).

To confirm the importance of ionic conductivity in the operation of LECs, we also fabricated sandwich-structured devices using thin films ( $\sim 0.4 \mu\text{m}$  thick) of the PPV and PEO blend as the active layer. No ionic species were added in the blend. These blend films were highly insulating (conductivity is less than  $10^{-9} \text{ S/cm}$ ). The electric current was less than 1  $\mu\text{A}$  even at bias up to 15 V. In addition, PPV and  $\text{LiCF}_3\text{SO}_3$  blend films ( $\sim 0.3 \mu\text{m}$  thick) were also used as the active layer. In this case, no PEO was added. The blend films also have low conductivity,  $3 \times 10^{-10} \text{ S/cm}$ .<sup>34</sup> The devices functioned like a typical ITO/PPV/Al light-emitting diode which turned-on at high voltage with low quantum efficiency.<sup>15a</sup> The current and light intensity at reverse bias were significantly lower than those in forward bias.

**5.4. Relaxation of the p–n Junction in LECs.** Since p-doped and n-doped PPVs have different chemical potentials, the biased LEC is a charged electrochemical cell. After the removal of the external bias, the doping profile changes, and the p–n junction relaxes as the cell discharges.

When the anode and cathode of an ITO/PPV + PEO/Al cell were disconnected (open-circuited) after continuous operation, light emission ceased immediately. A relatively large potential difference between the anode and cathode was measured, with the anode at a higher potential than the cathode. This open-circuit voltage decayed with time as shown in Figure 9. The voltage decreases slowly from 2.0 to 0.02 V in approximately 7 min. Between the intervals of 0 and 6 min, the decay is essentially exponential. Just as the formation rate of the p–n junction is determined by the slow ion transport, the relaxation rate is also limited by the ion mobility. While the p–n junction is relaxing, the excess lithium cations in the n-doped regime, as well as the excess trifluoromethanesulfonate anions in the p-doped regime, diffuse back into the electrolyte, restoring uniform (neutral) ionic charge throughout the polymer layer.

When the circuit is first opened, the instantaneous potential difference across the p–n junction should be the built-in potential 2.4 V (the band gap) rather than 2.0 V. In the surface cell LECs, we indeed measured open-circuit voltages as high as 2.3 V by applying a compensating voltage to the electrodes such that the *external* current remained zero during the relaxation of the p–n junction.

When the anode and cathode of the LEC were electrically shorted (through a low impedance ammeter) after a continuous

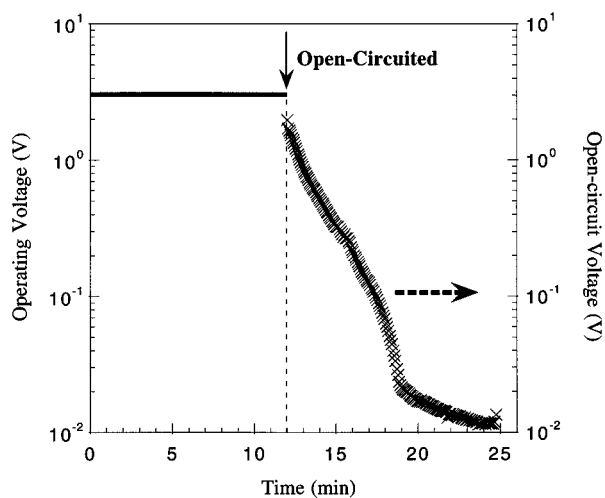


**Figure 9.** Decay of the open-circuit voltage of an ITO/PPV + PEO(Li)/Al cell after applying a 3 V bias for 12 min (ITO is the positive electrode).

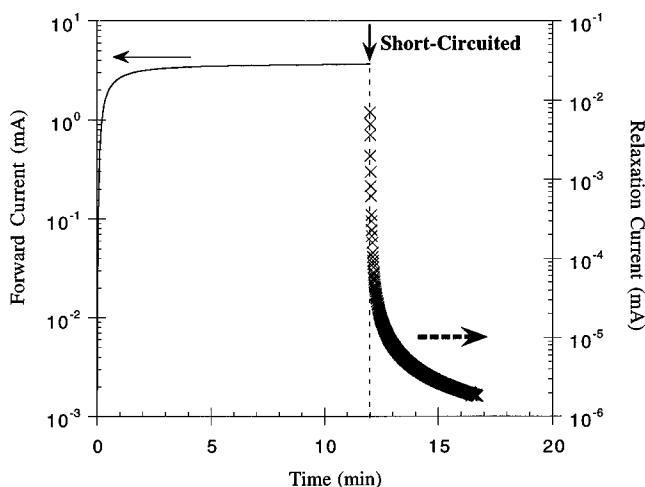


**Figure 10.** Chronoamperometric response at 3 V and the subsequent relaxation current at 0 V (short-circuited) of an ITO/PPV + PEO(Li)/Al cell. The relaxation current flows from ITO to Al.

operation, light emission ceased immediately. An electric current was detected flowing from the anode to the cathode, i.e., opposite to the charging current during formation of the junction. Figure 10 shows the decay of the zero-bias electric current (relaxation current) after the LEC had been continuously biased at 3 V for 12 min. Again, because there was some delay before the first data point of the relaxation current was taken, the actual initial current immediately after the circuit had been shorted was larger than 6  $\mu\text{A}$ .

As shown in Figure 10, the relaxation current decays very rapidly in the first minute, and then slows down and continues beyond 5 min. This relaxation current results from carrier transport between the p- and n-doped regions through the external wire. At the same time, there is also an internal current (not detectable by an external ammeter) between the p- and n-doped regimes. The total relaxation charge is the time integral of both the external and internal relaxation currents, which should equal the doping level of the p-doped and n-doped regimes. As discussed in section 2, however, with a low impedance meter in the external circuit, the internal current should be relatively unimportant. Using eq 2, we estimate  $Q \approx 8 \times 10^{-6} \text{ C}$ . From eq 3, the doping concentration was estimated to be  $\sim 0.7\%$  charges per phenylenevinylene unit,<sup>36</sup> consistent with the relatively small doping-induced spectral changes seen in Figure 8.

(34) Esteghamatian, M.; Xu, G. *Synth. Met.* **1994**, *63*, 195.

(35) Yu, G. US Patent Appl. No. 08/444998, 1995.

## 6. Conclusion

We have investigated the mechanism of operation of light-emitting electrochemical cells in which the active layer is a phase separated blend of conjugated polymer and polymer electrolyte. Devices made from PPV and PEO(LiCF<sub>3</sub>SO<sub>3</sub>) plus two contact electrodes constitute a novel solid-state light-emitting electrochemical cell. In this cell, a light-emitting p-n junction is created *in situ* through simultaneous p-type and n-type electrochemical doping of the luminescent PPV on opposite sides of the polymer layer. The admixed PEO(LiCF<sub>3</sub>SO<sub>3</sub>) complex provides the necessary counterions and ionic conductivity needed for electrochemical doping. During the doping process, the ionic species of the complex redistribute, so that in the established doping profile, cations dominate the n-doped regime and anions dominate the p-doped regime. The p-n junction is dynamic and reversible: its polarity may be reversed by applying a reverse voltage on the electrodes. The

---

(36) The density ( $d$ ) of the PPV and PEO blend film has been assumed to be 1 g/cm<sup>3</sup>. The number ( $N$ ) of phenylenevinylene units in the active area of the polymer layer is  $VdwA/M_{pv}$ , where  $V$  is the volume of the polymer layer,  $w$  is the weight percentage of PPV in the blend,  $A$  is Avogadro's number, and  $M_{pv}$  is the molar weight of phenylenevinylene.  $N$  is calculated to be  $6.6 \times 10^{15}$ .

(37) Zhang, C.; Braun, D.; Heeger, A. J. *J. Appl. Phys.* **1993**, *73*, 5177.

junction relaxes when the external bias is removed, and the semiconducting polymer PPV transforms back to the neutral nondoped state. Simultaneously, the ionic species redistribute, so that in the relaxed profile, a uniform neutral ion distribution is obtained. Bright green light is emitted from the p-n junction with a turn-on voltage close to the band gap of PPV. These devices are suitable for display applications, with initial results implying a relatively long storage life and stable continuous light emission at low driving voltages. The response speed of the light-emitting cells was around 1 s, depending on the diffusion of ions. It can be increased by increasing the ionic conductivity of the active polymer layer. Furthermore, once the light-emitting junction has been formed, the subsequent operation has electronic response which is fast (on the microsecond scale or faster).

**Acknowledgment.** We are grateful to Dr. Y. Cao, Dr. N. Colaneri, and Dr. P. Smith for numerous discussions. This work was supported by the National Science Foundation SBIR Grant No. 9361656 and by the Office of Naval Research.

**Supporting Information Available:** Color versions of Figures 1 and 7 are available on the World Wide Web.

JA953695Q